Available online at www.sciencedirect.com
SCIENCE DIRECT
Catalysis Today 114 (2006) 57–63
CATALYSIS TODAY
www.elsevier.com/locate/cattod

Effect of potassium and water vapor on the catalytic reaction of nitric oxide and dioxygen over platinum

S.S. Mulla [a], N. Chen [a], L. Cumaranatunge [a], W.N. Delgass [a], W.S. Epling [b,1], F.H. Ribeiro [a,*]

[a] *School of Chemical Engineering, Purdue University, Forney Hall of Chemical Engineering, 480 Stadium Mall Drive, West Lafayette, IN 47907-2100, United States*
[b] *Cummins Inc., 1900 McKinley Ave., Columbus, IN 47201, United States*

Available online 23 March 2006

Abstract

The turnover rate (TOR) per unit surface Pt atom for NO oxidation by O_2 on a $Pt/K/Al_2O_3$ NO_x storage-reduction catalyst was 2.5 times higher at 300 °C than the rate on a Pt/Al_2O_3 catalyst with the same Pt loading. The power rate law orders with respect to NO, O_2 and NO_2 on the $Pt/K/Al_2O_3$ catalyst were identical to those on Pt/Al_2O_3, viz. $r = k[NO]^1[O_2]^1[NO_2]^{-1}$, but the apparent activation energy obtained for the K-promoted catalyst was 60 kJ mol^{-1}, about 22 kJ mol^{-1} lower than on the Pt/Al_2O_3 catalyst. The presence of water vapor in the feed resulted in an initial and irreversible decrease in the Pt surface area and NO conversion for both $Pt/K/Al_2O_3$ and Pt/Al_2O_3 catalysts, but no changes in the reaction orders or apparent activation energy were observed. Water did not affect the NO oxidation turnover rates.

Keywords: Kinetics of NO oxidation on Pt; $Pt/K/Al_2O_3$; NO_2 inhibition of NO oxidation; Effect of water and potassium on NO oxidation on Pt

1. Introduction

Due to the increasingly stringent NO_x emission regulations imposed by the EPA [1], several research efforts are ongoing to understand the potential NO_x abatement techniques that are available for lean-burn diesel engines. One such approach is selective catalytic reduction (SCR) of NO_x in the engine exhaust with either unburned hydrocarbons (HC) from the fuel or with ammonia. It has been proposed that the oxidation of NO in the exhaust to NO_2 over noble metal sites substantially increases the rate and selectivity of HC-SCR [2–6].

Another approach for NO_x abatement is the NO_x storage/reduction (NSR) concept pioneered by Toyota for mobile applications [7]. The catalyst used for the NSR process has three essential parts: a supporting oxide, e.g., Al_2O_3; a noble metal that can catalyze oxidation and reduction reactions, e.g., Pt; and a NO_x storage component (typically alkali or alkaline earth metals), e.g., K or Ba. During lean operation, NO in the exhaust is oxidized to NO_2 over the noble metal component which then subsequently reacts with the storage component forming nitrates or nitrites. The oxidation of NO in the exhaust to NO_2 is found to substantially increase the NSR catalyst performance by enhancing NO_x storage [8–14]. As the trap saturates and loses its storage capacity it becomes necessary to regenerate it by providing a reducing atmosphere for a very short period, whereupon the stored NO_x is released and subsequently reduced over noble metal sites. The NSR catalyst is used with an engine that operates alternately under lean- and rich-burn conditions.

Additionally, the oxidation of NO to NO_2 is also a key reaction in the Continuously Regenerating Trap (CRT®) for soot removal [15]. In this case, the strong oxidizing nature of NO_2 is used to continuously oxidize the soot collected on a diesel particulate filter (DPF) at temperatures much lower than those required with oxygen alone. The NO_2 gets reduced to NO which is then re-oxidized to NO_2 over a Pt catalyst.

Thus, the oxidation of NO to NO_2 over Pt is an important step involved in all of the above mentioned processes. NO

* Corresponding author. Tel.: +1 765 494 7799; fax: +1 765 494 0805.
E-mail address: fabio@purdue.edu (F.H. Ribeiro).
[1] Present address: Department of Chemical Engineering, University of Waterloo, 200 University Ave. West, Waterloo, Ont., Canada N2L 3G1.

0920-5861/$ – see front matter © 2006 Elsevier B.V. All rights reserved.
doi:10.1016/j.cattod.2006.02.013

oxidation on supported Pt has been studied previously, but most authors did not consider the influence of the product NO_2 on the rate of oxidation of NO [16–24]. It has been shown recently that the oxidation of NO is inhibited by the reaction product NO_2 on Pt supported by both γ-Al_2O_3 [25] and SiO_2 [6].

The work presented here has been focused on understanding the NO oxidation step on a catalyst consisting of Pt and K phases on a γ-Al_2O_3 support. Both barium and potassium are known to be suitable storage elements of the NSR catalyst [26]. However, most studies concentrate on the Ba containing catalysts (for example, in Refs. [9–12,14,27–31]) with less information on K-based traps [32–35]. The main purpose of this work was to study the influence of potassium and water on the NO oxidation reaction. Water has been previously found to affect the overall trapping and reduction efficiency and also the rate of NO_x adsorption of NSR catalysts [33,36]. Therefore, it is important to quantify the effect of water, which is always present in the exhaust, on the oxidation of NO to NO_2.

2. Experimental methods

The Pt/Al_2O_3 and $Pt/K/Al_2O_3$ catalysts used in this study were supplied by EmeraChem in monolithic form. Based on a known liquid uptake of the bare monolith, the appropriate amount of γ-Al_2O_3 was mixed as an aqueous slurry. The bare monolith was dipped into this slurry, drained, dried and then calcined at 500 °C for 1 h. The monolith was then dipped into the Pt-containing aqueous solution such that a final Pt loading of approximately 50 g ft^{-3} of monolith was attained for both catalysts. The Pt salt precursor was amine-based. For the $Pt/K/Al_2O_3$ catalyst, potassium was further added using an aqueous solution of K_2CO_3.

Both monoliths had a length of 1 in., a cross-section of 60 channels with a cell density of 200 channels per $in.^2$. The percentage of metal exposed (PME) or metal dispersion, defined as the ratio of the number of surface Pt atoms to the total number of Pt atoms, was measured by H_2–O_2 titration [37] and was 42% for Pt/Al_2O_3 and 61% for $Pt/K/Al_2O_3$. The total sample weight was about 3 g with a Pt loading of ca. 0.3 wt% (per total catalyst weight) for both catalysts. The NO conversion for the NO oxidation reaction was measured in a bench-top, plug-flow stainless steel reactor. High-temperature Zetex insulation was wrapped around the catalyst sample and placed in the reactor tube. The insulation material blocked the space between the monolith and the wall of the reactor, minimizing the gas flow bypassing the catalyst. Glass beads were placed upstream of the catalyst sample to ensure mixing and uniformity of the gas flow, and the reactor was placed inside a temperature-controlled furnace. To minimize temperature gradients, the inlet gas was preheated before entering the reactor. Thermocouples were placed 6 mm before and after the catalyst sample to verify inlet and outlet gas temperatures. A reactor bypass loop after the preheater, and thus at the reactor conditions, was used to verify the nominal inlet concentrations of NO and NO_2 after each catalytic rate measurement. The gas phase rates were negligible as compared to the catalytic ones. All turnover rate calculations were done relative to the gas phase bypass concentrations, and hence reflected only the reaction over the catalyst and not the gas phase. In the experiments involving water in the feed gas, deionized water was metered by a water pump (Fluid Metering Inc., Model QVG50) and was vaporized in the preheater before entering the reactor. All the gas lines were heated to 120–150 °C. To avoid fluctuations in the water partial pressure, a 1.6 mm (0.0625 in.) diameter tube capillary with an internal diameter of 0.254 mm was used to deliver a continuous flow of water into the preheater. The NO and NO_x ($NO + NO_2$) concentrations in the outlet gas were detected with a chemiluminescence detector (California Analytical Instruments HCLD 400). The experiments were conducted with a total flow of approximately 6.6 L min^{-1}.

The NO oxidation apparent activation energy and reaction orders with respect to NO, O_2 and NO_2 were measured for Pt/Al_2O_3 and $Pt/K/Al_2O_3$ with and without water vapor in the feed gas. Before the experiments, both samples were pretreated at 150 °C with 10% O_2 in N_2 for 1 h followed by reduction with 0.5% H_2 in N_2 for 1.5 h with a constant total flow rate of 6.5 L min^{-1}. The reactor was operated in a differential manner by restricting the NO conversions to below 10% and by using excess NO_2 in the feed so that the contribution of the NO_2 formed to the total NO_2 concentration was negligible. The data reported here were taken after the catalyst was on stream for at least one hour. On the potassium containing NSR catalyst, this procedure ensured that the storage component is saturated with NO_x so that the NO_x storage process does not interfere with the NO oxidation kinetic measurements. Steady-state operation was further confirmed when, at the end of each experimental data set, the conditions of the first data point were replicated and reproducible results were obtained. Replication of the first data point also enabled us to monitor the deactivation of the catalysts with time-on-stream. For apparent activation energy tests, the temperature was varied between 237 and 360 °C in a random manner to minimize systematic errors affecting the data, while the feed composition (300 ppm NO, 170 ppm NO_2, 10% O_2, balance N_2) and the total flow rate (6.6 L min^{-1}) were kept constant. Similarly, to determine the effect of reactant and product concentrations on the NO oxidation rate, only the concentration of the species of interest was varied independently in a random manner, while keeping the concentrations of the other species and the temperature constant. The concentrations of the various species were varied over the following ranges: NO (90–450 ppm), O_2 (5–25%) and NO_2 (50–220 ppm). The errors in the apparent reaction orders and activation energies were calculated through a linear least-squares fit with 95% confidence intervals. The criteria suggested by Dekker et al. [38] were used to check external heat and mass transfer limitations. The Carberry number (Ca) and the parameter for external heat transfer limitation – given as $|(k_g(-\Delta H)C_b/hT_b)\gamma Ca|$, where k_g and h are extra-particle mass and heat transfer coefficients, respectively, C_b and T_b are steady-state bulk concentration and temperature, respectively, and $\gamma = E_a/RT_b$ – were of the order of 10^{-4} ($\ll 0.05$), suggesting negligible transport effects.

3. Results and discussion

3.1. NO oxidation on Pt/Al_2O_3

We recently published the kinetics of NO oxidation reaction on a Pt/Al_2O_3 catalyst [25] and will summarize the results here. The activation energy was found to be 82.6 kJ mol^{-1} (Fig. 1) and the power rate law orders were nearly +1 for both NO and O_2, and nearly −1 for NO_2 (Fig. 2). The following mechanism was proposed to explain the observed orders:

$$NO + * \overset{K_1}{\rightleftharpoons} NO^* \quad (1)$$

$$NO_2 + 2* \overset{K_2}{\rightleftharpoons} NO^* + O^* \quad (2)$$

$$O_2 + * \xrightarrow{k_3} O_2^* \quad (3)$$

$$O_2^* + * \xrightarrow{k_4} 2O^* \quad (4)$$

where * denotes a Pt site and K_i and k_i the equilibrium constant and the rate constant of the ith step, respectively. Step (3) was proposed as the rate determining step (RDS), and O^* the most abundant surface intermediate [18,23,30], with steps (1) and (2) in quasi-equilibrium. Note that step (2) is not an elementary step but is the combination of adsorption and reaction steps. Under the limiting condition of high O^* coverage, the rate expression takes the form

$$r = \left\{ \frac{k_3[L]K_1}{K_2} \right\} \frac{[NO][O_2]}{[NO_2]} \quad (5)$$

where [L] denotes the total surface concentration of active metal sites. Eq. (5) has the same concentration dependence (apparent reaction orders) as seen in our experiments.

Despres et al. [6] have also seen a similar product inhibition effect on NO oxidation by NO_2 on Pt/SiO_2. They reported a decrease in NO conversion and a concomitant increase in the NO oxidation differential rates with increasing NO feed concentrations up to about 500 ppm, with only NO and O_2 in the feed gas. This decrease in NO conversion with increasing

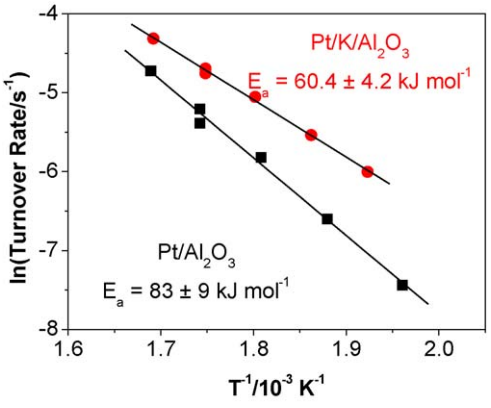

Fig. 1. Arrhenius plot for NO oxidation on Pt/Al_2O_3 and $Pt/K/Al_2O_3$ assuming a differential reactor. Feed: 300 ppm NO, 10% O_2, 170 ppm NO_2, balance N_2.

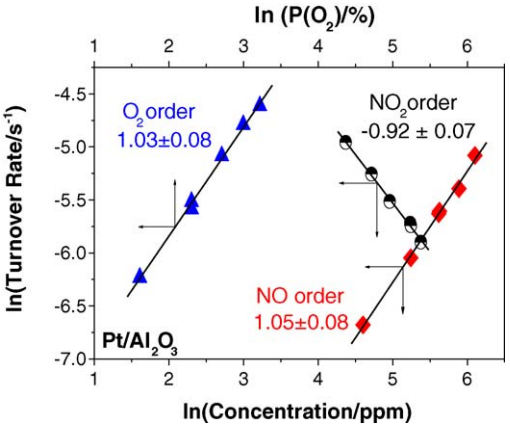

Fig. 2. NO oxidation turnover rate (TOR) dependence on O_2, NO and NO_2 concentrations at 300 °C for Pt/Al_2O_3. Feed for NO order: 170 ppm NO_2, 10% O_2, 100–450 ppm NO; feed for NO_2 order: 10% O_2, 300 ppm NO, 80–220 ppm NO_2; feed for O_2 order: 300 ppm NO, 170 ppm NO_2, 5–25% O_2. All feeds have N_2 as the balance gas.

NO feed concentrations may give the impression of inhibition by NO and hence appear to disagree with our results. However, these opposite trends in NO conversion and reaction rate with increasing NO feed concentrations can be explained with the help of the NO oxidation kinetic model we have described above and the equation for a plug-flow reactor. The derivation is not detailed here but in short, due to the NO_2 inhibition, the absence of excess NO_2 in the feed makes the measured rates a function of conversion even at the lowest measurable values of conversion, and this is reflected as NO appearing as an inhibitor even though the reaction order for NO is actually +1. Our model was tested against data sets in the literature. We used the NO conversion data as a function of temperature and NO, O_2 and NO_2 inlet concentrations given by Despres et al. [6] to fit the dependence of conversion to the concentrations of NO, O_2 and NO_2 based on our model. Their data fit our kinetic model with 98% confidence and give an apparent activation energy of ca. 86 kJ mol^{-1}, close to our findings. However, we could not explain all the results reported by Despres et al. [6]. For example, they observed that their oxidation rates leveled off at inlet O_2 concentrations above 10%, whereas our results show first order dependence on O_2 concentrations up to 25% (Fig. 2). Using the NO or NO_2 outlet concentrations versus temperature data given by Olsson et al. [18] and Crocoll et al. [23] on a Pt/Al_2O_3 catalyst with only NO and O_2 in the inflow also allowed us to calculate, using our model, an apparent activation energy of ca. 80 kJ mol^{-1}.

We were also able to compare turnover rates but with the caveat that the rates are a function of Pt particle size. A compilation of the rate data in the literature obtained by integrating the data provided in the original papers using our kinetic model and correcting to our reaction conditions is shown in Table 1. Our TOR fits well with the observed trend of increasing rate with increasing Pt particle size [16,19,39–41].

We had also noted in our previous work [25] that not accounting for the inhibition of NO_2 would make the apparent activation energy (E_a) (obtained from the slope of ln TOR versus $1/T$ for differential conversions) appear to be half its

Table 1
Literature values for turnover rates of NO oxidation to NO_2 on Pt

Catalyst	Pt loading (wt%)	Pt particle size[a] (nm)	Turnover rate[b] ($\times 10^{-2}$ s^{-1})	Ref.
Pt/Al_2O_3	0.27	1.2	0.23	[16]
Pt/Al_2O_3	0.3	2.4	0.35	This work
Pt/SiO_2	2.5	7	4.2[c]	[6]
Pt/Al_2O_3	2.3	22	16	[18]
Pt/Al_2O_3	2	200	25	[23]

[a] Calculated using d (nm) = 1/(Pt dispersion), except for Refs. [6,23].
[b] Rates per unit of surface Pt atom corrected to 300 °C, 300 ppm NO, 170 ppm NO_2, 10% O_2, balance N_2.
[c] 5% water was also present in the feed.

actual value. If one does not know about the inhibitory effect by NO_2, the value of the apparent rate constant (k) will be changing not only due to temperature but also because of NO_2 concentration. One would be plotting $k/[NO_2]$ at each point in an Arrhenius plot. The slope would of course not be an apparent activation energy in this case, but the value of the slope would be one half of the actual apparent activation energy value. This however does not imply that the apparent activation energy depends on NO_2 feed concentration, but is simply an outcome of the mathematical relationship between TOR and temperature detailed in our previous work [25]. Mei et al. [42] carried out kinetic Monte Carlo simulation of NO_2 formation with only NO and O_2 in the inlet and found a simulated activation energy of 37.6 kJ mol^{-1} on Pt(1 0 0). This value is indeed approximately half of the actual E_a we reported and moreover, matches well with the value of 39 kJ mol^{-1} we observed experimentally from the slope of ln TOR versus $1/T$ with only NO and O_2 in the feed gas [25].

3.2. Effect of potassium

The variation of the NO oxidation reaction rate with temperature over $Pt/K/Al_2O_3$ catalyst is shown in Fig. 1. The rates are expressed as turnover rates (TOR), defined as moles of NO reacted per second per mole of surface Pt. The forward rates (r_f) were calculated from the measured overall rates (r_{ov}) using the expression:

$$r_{ov} = r_f(1 - \beta) \tag{6}$$

where β is the approach to equilibrium given as:

$$\beta = \frac{[NO_2]}{K[NO][O_2]^{1/2}} \tag{7}$$

with K as the equilibrium constant. The β values in our experiments ranged from 0.02 to 0.17, indicating that the reaction was away from equilibrium. The apparent activation energies (E_a) for both Pt/Al_2O_3 and $Pt/K/Al_2O_3$ catalysts are given in Table 2.

Fig. 3 shows the effects of reactant and product concentrations on the NO oxidation turnover rate at 300 °C for $Pt/K/Al_2O_3$ catalyst. The results are summarized in Table 2. Similar to the Pt/Al_2O_3 catalyst, the rate of NO oxidation had a nearly first order dependence with respect to the reactants NO and O_2, while it was close to negative first order with respect to the product NO_2 over the concentration range studied. Thus, NO_2 was found to inhibit NO oxidation on the K containing NSR catalyst as well.

For comparison, NO oxidation turnover rates on Pt/Al_2O_3 and $Pt/K/Al_2O_3$ catalysts under the same reaction conditions are reported in Table 2. The TOR was found to be higher on the $Pt/K/Al_2O_3$ catalyst. At the standard condition (300 °C, 300 ppm NO, 10% O_2, 170 ppm NO_2), the TOR on the $Pt/K/Al_2O_3$ catalyst was about 2.5 times higher than that on the Pt/Al_2O_3 catalyst. Considering that the $Pt/K/Al_2O_3$ catalyst had a higher Pt dispersion (61% compared to 42% for Pt/Al_2O_3), or equivalently, and possibly a smaller Pt particle size than the Pt/Al_2O_3 catalyst and the fact that larger Pt particles exhibit higher turnover rates for NO oxidation than smaller particles [16,19,39–41], the increase in the TOR observed on our $Pt/K/Al_2O_3$ catalyst is indicative of an effect of K on Pt/Al_2O_3 for the NO oxidation reaction. In a similar study, Olsson et al. [30] reported a lower NO_2 production rate for their $Pt/BaO/Al_2O_3$ catalyst in comparison to a Pt/Al_2O_3 catalyst based on the total Pt content of the catalysts. They quoted a five times lower Pt dispersion on the BaO containing catalyst as a possible reason for the observed decrease in the rate per unit weight of Pt. However, upon converting their NO_2 production rate (mol s^{-1} mg^{-1} of Pt) to turnover rate per unit of surface Pt atom, we found that their BaO based NSR catalyst also yields a TOR about 2.5 times higher than their Pt/Al_2O_3 catalyst at 300 °C.

The promotional effect of K on Pt for a variety of reactions has been observed by many researchers in the field [43–45]

Table 2
Summary of the NO oxidation reaction kinetics on Pt/Al_2O_3 and $Pt/K/Al_2O_3$ catalysts in the absence of water vapor

Catalyst	PME (%)	E_a (kJ mol^{-1})	NO order	O_2 order	NO_2 order	TOR[a] (s^{-1})
Pt/Al_2O_3	42	82.6 ± 9	1.05 ± 0.08	1.03 ± 0.08	-0.92 ± 0.07	3.5×10^{-3}
$Pt/K/Al_2O_3$	61	60.4 ± 4.2	1.03 ± 0.08	0.95 ± 0.08	-0.96 ± 0.1	8.6×10^{-3}

[a] TOR at 300 °C, 300 ppm NO, 10% O_2, 170 ppm NO_2, balance N_2.

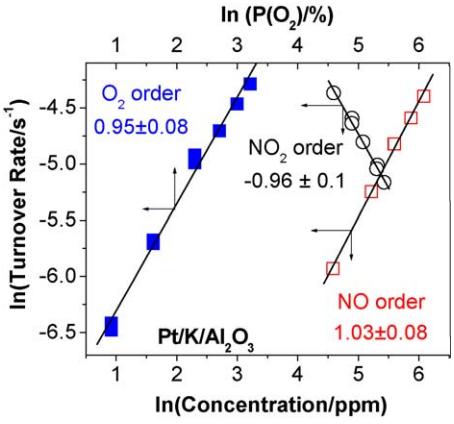

Fig. 3. NO oxidation turnover rate (TOR) dependence on O_2, NO and NO_2 concentrations at 300 °C for $Pt/K/Al_2O_3$. Feed for NO order: 170 ppm NO_2, 10% O_2, 100–440 ppm NO; feed for NO_2 order: 10% O_2, 300 ppm NO, 100–230 ppm NO_2; feed for O_2 order: 300 ppm NO, 170 ppm NO_2, 5–25% O_2. All feeds have N_2 as the balance gas.

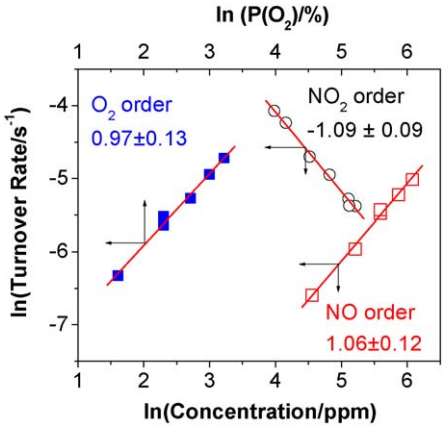

Fig. 4. NO oxidation reaction orders at 300 °C in presence of 5% water vapor for Pt/Al_2O_3. Feed for NO order: 170 ppm NO_2, 10% O_2, 5% H_2O, 100–440 ppm NO; feed for NO_2 order: 10% O_2, 300 ppm NO, 5% H_2O, 50–180 ppm NO_2; feed for O_2 order: 300 ppm NO, 170 ppm NO_2, 5% H_2O, 5–25% O_2. All feeds have N_2 as the balance gas.

using single crystal model catalysts but K was in metallic form. In our case K will be in oxidized form since the catalyst was exposed to the atmosphere. Adsorption of molecular oxygen (step (3) above) was previously identified as the rate determining step for NO oxidation [25] and hence, an increase in the rate of O_2 adsorption on $Pt/K/Al_2O_3$ could possibly explain the increase in the NO oxidation turnover rate we observe. Minemura et al. [46] also quoted increased O_2 adsorption as a possible reason for CO oxidation promotion they observed on their $Pt/K/Al_2O_3$ catalyst. The promotional effect of K on NO oxidation over Pt is not understood.

3.3. Effect of water vapor

To investigate the effect of water, 5% water vapor was added to the feed gas and the reaction orders and activation energies were measured on both Pt/Al_2O_3 and $Pt/K/Al_2O_3$ catalysts. No appreciable change in E_a or apparent reaction orders with respect to any of the reactant or product species was observed, indicating that the reaction kinetics were not altered in the presence of water. The results are summarized in Table 3. Figs. 4 and 5 show the reaction orders with 5% water vapor in the feed gas for Pt/Al_2O_3 and $Pt/K/Al_2O_3$, respectively. It was found however, that the presence of water caused the NO conversion to decrease on both catalysts. For Pt/Al_2O_3, the conversion decreased by a factor of about 3 whereas on $Pt/K/Al_2O_3$ the conversion was about 1.4 times lower, relative to the dry conditions discussed earlier and as shown in Table 4.

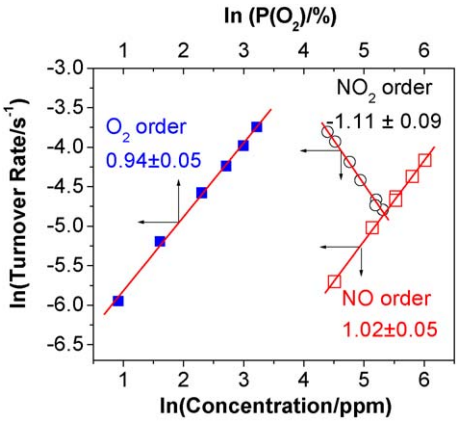

Fig. 5. NO oxidation reaction orders at 300 °C in presence of 5% water vapor for $Pt/K/Al_2O_3$. Feed for NO order: 170 ppm NO_2, 10% O_2, 5% H_2O, 90–410 ppm NO; feed for NO_2 order: 10% O_2, 300 ppm NO, 5% H_2O, 80–200 ppm NO_2; feed for O_2 order: 300 ppm NO, 170 ppm NO_2, 5% H_2O, 5–25% O_2. All feeds have N_2 as the balance gas.

Moreover, this decrease in conversion, which only occurred during the first contact of the sample with water, was irreversible since the removal of water from the feed gas did not result in the recovery of the initial conversions obtained prior to the addition of water to the feed. The NO conversions after removal of water from the feed remained nearly at the same lower values observed in the experiments that contained 5% H_2O in the feed (Table 4). In other words, the first contact of

Table 3
Summary of the NO oxidation reaction kinetics on Pt/Al_2O_3 and $Pt/K/Al_2O_3$ catalysts in presence of 5% water

Catalyst	PME[a] (%)	E_a (kJ mol^{-1})	NO order	O_2 order	NO_2 order	TOR[b] (s^{-1})
Pt/Al_2O_3	14	82.5 ± 9.4	1.06 ± 0.12	0.97 ± 0.13	−1.09 ± 0.09	3.4×10^{-3}
$Pt/K/Al_2O_3$	44	64.8 ± 4.2	1.02 ± 0.05	0.94 ± 0.05	−1.11 ± 0.09	8.6×10^{-3}

[a] PME based on CO oxidation results after the removal of water from feed.
[b] TOR at 300 °C, 300 ppm NO, 10% O_2, 170 ppm NO_2, 5% H_2O, balance N_2.

Table 4
Comparison of NO and CO conversions before and after exposure to 5% H_2O on Pt/Al_2O_3 and $Pt/K/Al_2O_3$

	Pt/Al_2O_3		$Pt/K/Al_2O_3$	
	NO conversion[a] (%)	CO conversion[b] (%)	NO conversion[a] (%)	CO conversion[b] (%)
Before water exposure	4.4	9.9	11.1	2.0
Add 5% H_2O	1.5	–	8.2	–
Continue with no water exposure	1.4	3.2	7.9	1.4

[a] NO conversion at 300 °C, 300 ppm NO, 10% O_2, 170 ppm NO_2, 0 or 5% H_2O, balance N_2.
[b] CO conversion at 160 °C, 1% CO, 5% O_2, balance N_2.

the catalysts with water caused the NO conversion to decrease, and thereafter, the conversion remained nearly at that stable lower level, irrespective of the presence or absence of water in the inflow. Similar irreversible water inhibition effects were observed by Olsson et al. [47] for their Pt/Al_2O_3 catalyst. Crocoll et al. [23] also found their NO conversion to decrease for their Pt/Al_2O_3 catalyst in the presence of 6% H_2O in the feed gas.

We further investigated this inhibitory effect of water by using the CO oxidation reaction as a tool to determine if there was any change in the Pt surface area due to the exposure to water. The structure insensitivity of CO oxidation over Pt [48,49] makes it an alternative technique to measure the relative Pt surface area of these catalysts without performing the conventional H_2–O_2 chemisorption measurements, which require that the monolith sample be crushed during sample pretreatment making the catalyst unusable for further reaction experiments. When the CO oxidation reaction was performed on Pt/Al_2O_3 and $Pt/K/Al_2O_3$ catalysts before and after they had been exposed to 5% water vapor, it was found that at 160 °C with 1% CO, 5% O_2 and balance N_2 in the feed gas, the CO conversions decreased by nearly the same factors as seen for NO oxidation on the two catalysts, viz. about 3 times lower for Pt/Al_2O_3 and about 1.4 times lower for $Pt/K/Al_2O_3$ as shown in Table 4. This decrease in the CO conversions can thus be taken as an indication of permanent loss of Pt surface area due to the exposure to the wet environment. Thus, it seems that once the Pt/Al_2O_3 and $Pt/K/Al_2O_3$ samples have been exposed to a water-containing atmosphere, there is an irreversible change in the Pt surface area which results in a loss in NO oxidation performance, but no apparent change in the reaction kinetics. Clearly then, the turnover rates on the two catalysts normalized by the corresponding Pt surface area before and after water exposure (the surface Pt moles after water exposure being calculated from CO oxidation results) should be identical, and indeed they are as shown in Figs. 6 and 7 for Pt/Al_2O_3 and $Pt/K/Al_2O_3$ catalysts, respectively.

However, the results presented here do not provide a mechanism on how water causes a permanent loss of surface Pt sites and a subsequent decrease in NO conversion. It cannot be due to the sintering of the Pt particles, since that would have increased the NO oxidation TOR because of the larger Pt particles, whereas we did not observe any changes in the turnover rates. Zhu et al. [50] have attributed the deactivation of their Pd/SiO_2 catalyst for complete methane oxidation to the migration of oxidized silicon caused by water resulting in the blocking of the active sites. They suggest that interaction of silica with water results in a mobile species that migrates to the palladium particle surface and hence covers the active Pd site. Although the catalysts used in this present study were supported on alumina, silica is a common contaminant in catalyst supports. Therefore, it can be postulated that the water caused

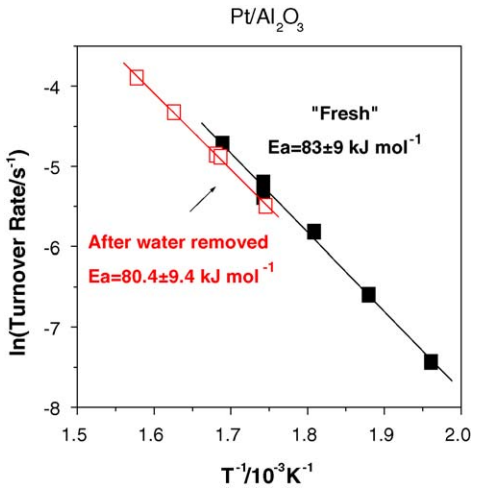

Fig. 6. Comparison of NO oxidation turnover rates (TOR) before and after exposure to 5% H_2O on Pt/Al_2O_3. The Pt surface area after exposure to 5% H_2O is about three times lower as indicated by CO oxidation results. Experimental conditions as in Fig. 1.

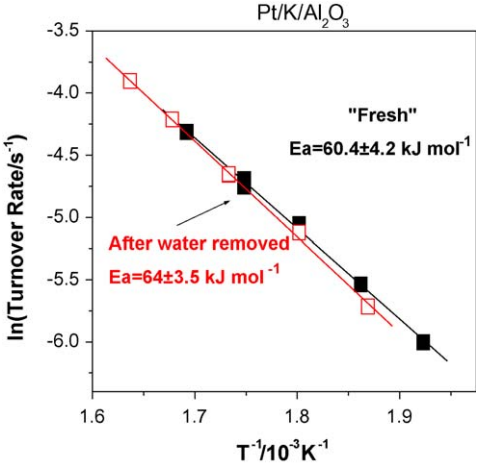

Fig. 7. Comparison of NO oxidation turnover rates (TOR) before and after exposure to 5% H_2O on $Pt/K/Al_2O_3$. The Pt surface area after exposure to 5% H_2O is about 1.4 times lower as indicated by CO oxidation results. Experimental conditions as in Fig. 1.

the migration of silica or some other impurity from the support to the active Pt sites and resulted in the deactivation seen in this NO oxidation study. Zhu et al. [50] also concluded that silica is not a good support for reactions where water is present based on the catalyst deactivation they observed. Silica has been found to be a better support than alumina for both NO oxidation [19,24,39] and HC-SCR [51,52], but in the absence of water. It would, therefore, be interesting to study the support effects on these reactions in the presence of water, especially since water is inevitable in the engine exhaust.

4. Conclusions

The kinetics of NO oxidation for a K-containing Pt/Al_2O_3 catalyst were investigated and compared to a conventional Pt/Al_2O_3 catalyst. Similar to the Pt/Al_2O_3 catalyst, the forward rate of NO_2 production on the $Pt/K/Al_2O_3$ catalyst was nearly first order with respect to both NO and O_2 concentrations and negative first order with respect to the NO_2 concentration. However, a lower apparent activation energy was observed for the $Pt/K/Al_2O_3$ catalyst (60 kJ mol^{-1}) compared to the Pt/Al_2O_3 catalyst (82 kJ mol^{-1}). The turnover rate was also higher on the $Pt/K/Al_2O_3$ catalyst. This promotional effect of K on Pt was only by a factor of about 2 at 300 °C and it may be attributed to the enhanced rate of O_2 adsorption on the $Pt/K/Al_2O_3$ surface which we suggested as the rate determining step in the kinetic model proposed for NO oxidation. The effect of H_2O, one of the primary exhaust gas components, on NO oxidation on both $Pt/K/Al_2O_3$ and Pt/Al_2O_3 was also investigated. The presence of water vapor in the feed caused an initial and irreversible decrease in the active Pt surface area and a corresponding loss in NO conversion, but no change in the TOR or reaction kinetics, for both $Pt/K/Al_2O_3$ and Pt/Al_2O_3 catalysts. The blocking of the Pt sites caused possibly by the migration of impurities from the support is believed to be the cause of this poisoning by water.

Acknowledgments

We thank the Indiana 21st Century Research and Technology Fund and Cummins Inc. for financial support of this work. The authors would also like to acknowledge the Department of Energy (CRADA ORNL97-0489) for support.

References

[1] Control of Air Pollution from New Motor Vehicles: Heavy-Duty Engine and Vehicle Standards and Highway Diesel Fuel Sulfur Control Requirements, U.S. EPA, 40 CFR Parts 69, 80 and 86.
[2] R. Burch, J.A. Sullivan, T.C. Watling, Catal. Today 42 (1998) 13.
[3] C. Yokoyama, M. Misono, J. Catal. 150 (1994) 9.
[4] H. Hamada, Y. Kintaichi, M. Inaba, M. Tabata, T. Yoshinari, H. Tsuchida, Catal. Today 29 (1996) 53.
[5] H. Ohtsuka, Appl. Catal. B 33 (2001) 325.
[6] J. Despres, M. Elsener, M. Koebel, O. Kroecher, B. Schnyder, A. Wokaun, Appl. Catal. B 50 (2004) 73.
[7] N. Takahashi, H. Shinjoh, T. Iijima, T. Suzuki, K. Yamazaki, K. Yokota, H. Suzuki, N. Miyoshi, S.-i. Matsumoto, et al. Catal. Today 27 (1996) 63.
[8] W.S. Epling, L.E. Campbell, A. Yezerets, N.W. Currier, J.E. Parks, Catal. Rev. 46 (2004) 163.
[9] K.S. Kabin, R.L. Muncrief, M.P. Harold, Y. Li, Chem. Eng. Sci. 59 (2004) 5319.
[10] S. Salasc, M. Skoglundh, E. Fridell, Appl. Catal. B 36 (2002) 145.
[11] H. Mahzoul, J.F. Brilhac, P. Gilot, Appl. Catal. B 20 (1999) 47.
[12] F. Prinetto, G. Ghiotti, I. Nova, L. Lietti, E. Tronconi, P. Forzatti, J. Phys. Chem. B 105 (2001) 12732.
[13] S. Kikuyama, I. Matsukuma, R. Kikuchi, K. Sasaki, K. Eguchi, Appl. Catal. A 226 (2002) 23.
[14] P.J. Schmitz, R.J. Baird, J. Phys. Chem. B 106 (2002) 4172.
[15] B.J. Cooper, H.J. Jung, J.E. Thos, US Patent 4,902,487 (1990).
[16] J.-H. Lee, H.H. Kung, Catal. Lett. 51 (1998) 1.
[17] R. Burch, T.C. Watling, J. Catal. 169 (1997) 45.
[18] L. Olsson, B. Westerberg, H. Persson, E. Fridell, M. Skoglundh, B. Andersson, J. Phys. Chem. B 103 (1999) 10433.
[19] E. Xue, K. Seshan, J.R.H. Ross, Appl. Catal. B 11 (1996) 65.
[20] E. Xue, K. Seshan, J.G. van Ommen, J.R.H. Ross, Appl. Catal. B 2 (1993) 183.
[21] G. Corro, M.P. Elizalde, A. Velasco, React. Kinet. Catal. Lett. 76 (2002) 117.
[22] L.D. Kieken, M. Neurock, D. Mei, J. Phys. Chem. B 109 (2005) 2234.
[23] M. Crocoll, S. Kureti, W. Weisweiler, J. Catal. 229 (2005) 480.
[24] J. Oi-Uchisawa, A. Obuchi, R. Enomoto, S. Liu, T. Nanba, S. Kushiyama, Appl. Catal. B 26 (2000) 17.
[25] S.S. Mulla, N. Chen, W.N. Delgass, W.S. Epling, F.H. Ribeiro, Catal. Lett. 100 (2005) 267.
[26] M. Takeuchi, S.i. Matsumoto, Top. Catal. 28 (2004) 151.
[27] J.A. Anderson, A.J. Paterson, M. Fernandez-Garcia, Stud. Surf. Sci. Catal. 130B (2000) 1331.
[28] E. Fridell, M. Skoglundh, B. Westerberg, S. Johansson, G. Smedler, J. Catal. 183 (1999) 196.
[29] I. Nova, L. Castoldi, L. Lietti, E. Tronconi, P. Forzatti, Catal. Today 75 (2002) 431.
[30] L. Olsson, H. Persson, E. Fridell, M. Skoglundh, B. Andersson, J. Phys. Chem. B 105 (2001) 6895.
[31] R.L. Muncrief, P. Khanna, K.S. Kabin, M.P. Harold, Catal. Today 98 (2004) 393.
[32] C.S. Daw, K.E. Lenox, K. Chakravarthy, W.E. Epling, G. Campbell, Int. J. Chem. Reactor Eng. 1 (2003) A24.
[33] T.J. Toops, D.B. Smith, W.S. Epling, J.E. Parks, W.P. Partridge, Appl. Catal. B 58 (2005) 255.
[34] T.J. Toops, D.B. Smith, W.P. Partridge, Appl. Catal. B 58 (2005) 245.
[35] L.J. Gill, P.G. Blakeman, M.V. Twigg, A.P. Walker, Top. Catal. 28 (2004) 157.
[36] W.S. Epling, G.C. Campbell, J.E. Parks, Catal. Lett. 90 (2003) 45.
[37] J.E. Benson, M. Boudart, J. Catal. 4 (1965) 704.
[38] F.H.M. Dekker, A. Bliek, F. Kapteijn, J.A. Moulijn, Chem. Eng. Sci. 50 (1995) 3573.
[39] S. Benard, L. Retailleau, F. Gaillard, P. Vernoux, A. Giroir-Fendler, Appl. Catal. B 55 (2005) 11.
[40] L. Olsson, E. Fridell, J. Catal. 210 (2002) 340.
[41] P. Denton, A. Giroir-Fendler, H. Praliaud, M. Primet, J. Catal. 189 (2000) 410.
[42] D. Mei, Q. Ge, M. Neurock, L. Kieken, J. Lerou, Mol. Phys. 102 (2004) 361.
[43] G. Pirug, H.P. Bonzel, G. Broden, Surf. Sci. 122 (1982) 1.
[44] E.L. Garfunkel, G.A. Somorjai, Surf. Sci. 115 (1982) 441.
[45] J.C. Bertolini, P. Delichere, J. Massardier, Surf. Sci. 160 (1985) 531.
[46] Y. Minemura, S. Ito, T. Miyao, S. Naito, K. Tomishige, K. Kunimori, Chem. Commun. 11 (2005) 1429.
[47] L. Olsson, M. Abul-Milh, H. Karlsson, E. Jobson, P. Thormaehlen, A. Hinz, Top. Catal. 30/31 (2004) 85.
[48] P.J. Berlowitz, C.H.F. Peden, D.W. Goodman, J. Phys. Chem. 92 (1988) 5213.
[49] M. Boudart, G. Djega-Mariadassou, Kinetics of Heterogeneous Catalytic Reactions, Princeton University Press, Princeton, NJ, 1984, p. 190.
[50] G. Zhu, K.-I. Fujimoto, D.Y. Zemlyanov, A.K. Datye, F.H. Ribeiro, J. Catal. 225 (2004) 170.
[51] R. Burch, T.C. Watling, Catal. Lett. 43 (1997) 19.
[52] R. Burch, P.J. Millington, Catal. Today 29 (1996) 37.